# PIV Investigation of the Flow Characteristics in 2-leg Internal Coolant Passages of Gas Turbine Airfoils with Film Cooling Hole Ejection

**D. Chanteloup, A. Bölcs**

Laboratoire de Thermique appliquée et de Turbomachines (LTT)
Département Génie Mécanique (DGM)
Swiss Federal Institute of Technology (EPFL)
1015 Lausanne, Switzerland
denis.chanteloup@epfl.ch ; albin.boelcs@epfl.ch

**Abstract**: *A study of flow in two stationary models of two-pass internal coolant passages is presented, which focuses on the flow characteristics in the 180-deg bend region, and downstream of the bend, where the flow is redeveloping. A stereoscopic digital PIV system measured all three velocity-components simultaneously to obtain mean-velocity, and turbulence quantities of the flow field. The coolant passage model consisted of two square passages, each having a 20 hydraulic diameter length, separated by a rounded-tip web of 0.2 passage widths, and connected by a sharp 180 deg bend with a rectangular outer wall. Ribs were mounted on the bottom and top walls of both legs, with a staggered arrangement, and at 45 deg to the flow. The rib height and spacing were 0.1 and 1.0 passage heights, respectively. The measurements were obtained for a flow condition, with a Reynolds number of 50,000. The geometries are similar in both sections except for one, which is equipped with extraction holes to simulate holes for film cooling. Two series of holes are placed solely in the bottom wall, 4 holes are located in the bend, and 12 in the downstream leg. The global extraction through the holes was set to 50% of the inlet massflow. This paper presents new measurements of the flow in the straight legs, as well as in the bend of the passage equipped with holes, detailed comparison of the flow upstream, inside and downstream of the bend region between both configurations, and the effects of extraction inside the cooling channels.*

## 1. NOMENCLATURE

- X Cartesian coordinate in axial duct direction
- Y Cartesian coordinate in cross duct direction
- Z Cartesian coordinate in horizontal duct direction
- $\theta$ Cylindrical coordinate in streamwise direction
- r Cylindrical coordinate in radial direction
- U Mean velocity component in x direction
- V Mean velocity component in y direction
- W Mean velocity component in z direction
- $U_\theta$ Mean velocity component in streamwise direction in bend
- $U_r$ Mean velocity component in radial direction in bend
- u' Fluctuating velocity component in axial direction
- v' Fluctuating velocity component in cross duct direction
- w' Fluctuating velocity component in vertical direction
- $u'_\theta$ Fluctuating velocity component in streamwise direction
- $u'_r$ Fluctuating velocity component in radial direction
- $U_b$ Bulk mean-velocity
- L Test section length
- D Height and width of passage legs, D=100 mm
- $D_h$ Hydraulic diameter $D_h$=D
- B Thickness of divider plate
- P Rib pitch
- e Rib height
- S Section length in bend at 90° section
- k Turbulent kinetic energy

$$\frac{\frac{1}{2}\left(\left(u'^2+v'^2+w'^2\right)\right)}{U_b^2} \Leftrightarrow \frac{\frac{1}{2}\left(\left(u_\theta'^2+u_r'^2+v'^2\right)\right)}{U_b^2} \quad \textit{in bend}$$

## 2. INTRODUCTION

For the design of gas turbine blades, a detailed knowledge of the physical phenomena in the passage is necessary. Although CFD simulations can provide a better understanding of these phenomena, the numerical heat transfer predictions are not yet sufficiently accurate for design purposes. To improve the performance of the CFD codes, a validation of the predictions is necessary and detailed measurements of the flow structure in the passages are required for comparison.

[1] measured local heat transfer coefficients around the entrance to a normal hole. They reported considerable heat transfer coefficient variations (six times the plain duct local value) around the entrance. [2] noted that in presence of normal ribs, the heat transfer in the vicinity of the holes was increased of about 25%. Although detailed heat transfer measurements in coolant channels with film cooling holes are available in the literature, the flow in such ducts hasn't been described to the authors knowledge.

In the present study, the particle-image-velocimetry (PIV) method was employed for the investigation of the flow field in models of a stationary two-pass coolant passage. The out-of-motion of the tracers (perpendicular to the light sheet plane) produces a systematic measurement error depending on the distance from the optical axis, e.g. [3]. This measurement error can be avoided by using a stereoscopic PIV setup ([4], [5]). A stereoscopic digital PIV system, based on the angular displacement method, was used for the present investigation ([6]). This PIV system is capable of simultaneously measuring all three velocity-components. Subsequently, an ensemble average of the velocity data in identical spatial windows is calculated to determine the mean and fluctuating velocity field.

This paper presents initial results from the Brite-Euram project for Internal Cooling of Turbine Blades (ICTB) measured with a PIV system. The objective of [7] was to present results in a base configuration and to determine the influence of the rib placement in the near bend regions on the flow fields upstream, inside, and downstream of the bend, and to provide new measurements of developed flow between ribs. The specific objectives of the present paper are to determine the influence of a flow extraction through simulating film-cooling holes, in the cooling channel 180deg turn vicinity.

## 3. EXPERIMENTAL SETUP

### *1. Test Facility*

A sketch of the test section is shown in Figure 1. Air was the working medium and was supplied by a continuously running compressor.

Both studied configurations have the same inner geometry characteristics. The baseline configuration test section is a two-pass, cooling passage model of a gas turbine blade. The flow path in the downstream and upstream passages has a cross-section of 100*100mm$^2$ with a corresponding hydraulic diameter, $D_H = 100mm$, and a length of $20D_H$. The outer walls of the test section are made of 5-mm-thick

extruded Plexiglas to obtain good optical properties for the PIV experiment. In the straight-corner bend, the clearance between the tip of the divider plate and the outer wall is equal to 1 $D_h$. The thickness of the divider plate or web between the two passages is $0.2D_H$. The tip of the divider plate is cylindrically shaped with a $0.1D_H$ radius. Square ribs with an angle of 45 deg to the passage centreline, rib heights of 0.1 hydraulic diameters ($e/D_H = 0.1$), and rib spacing of 10 rib heights ($P/e = 10$) are mounted in a staggered arrangement on the top and bottom wall of the passage. The ribs in the bend region and the dimensions of the bend are shown in Figure 1. Eighteen ribs are mounted on each of the top and bottom walls in each of the upstream and downstream passages of the model (18 * 4). The second configuration also called the *hole* configuration, has two series of holes for film cooling simulation. It has been chosen to place these holes solely in the bottom wall. The total mass flow through the holes is 50% of the mass flow in the test model, leading to a hole pitch to hole diameter ratio of 6. The first series of holes is placed in the bend region, $0.2D_H$ apart from the end wall. 4 $0.073D_H$-diameter holes are equally displaced between the leading and the trailing outer walls. 12 0.082*DH*-diameter holes are located downstream of the bend, the rib pitch to hole pitch ratio is set to 2, in order to have two holes per rib-pitch. This series is situated on the bottom wall downstream leg centreline (*Z*=-0.6).

A modular concept was chosen for the test section that allows an easy exchange of the components. The total model test section including the test section entrance is turned 90 deg around the x-axis to obtain additional measurement planes without changing the flow conditions in the passage.

## 2. ***Flow conditions, measurement program and coordinate systems***

The measurements were obtained with air as working medium, at a flow Reynolds number of 50,000 (corresponding to a bulk velocity: $Ub = 7.58m/s$), at the entrance of the test section. The Reynolds number is based on the 0.1 m hydraulic diameter with an air temperature of 20 C. Upstream of the test-rig, the mass flow is measured by means of a 5864S Brooks flow meter with a 1-percent accuracy. The turbulence level is approximately 3 percent at the model inlet.

Extraction through the holes is adjusted by increasing the inner configuration pressure level. A butterfly valve, placed far downstream of the test section exit, adjusts the backpressure. A second 5864S Brooks flow meter, measures the exit massflow downstream of the butterfly valve, allowing to adjust a 50% $Q_{in}$ extraction.

Detailed measurements of the flow structure in the passage have been obtained in the bend, upstream ($3D_H$) and downstream ($4D_H$) of the 180 deg bend. The definition of the coordinate systems in the test facility is shown in Figure 1. A Cartesian coordinate system is used for the straight passages and a cylindrical coordinate system is used for the bend region. The origin for both coordinate systems is set on the bottom wall at the centre of the rounded end of the divider plate for both coordinate systems. In the Cartesian (*X, Y, Z)* system, *X* is defined as positive in the streamwise direction of the flow downstream of the bend exit, *Y* is defined positive vertically upwards in the horizontal test section orientation, and *Z* is defined as shown. In the

cylindrical ($\theta$, $r$, $Y$) coordinate system, the radial component r is defined as positive in the direction towards the outer wall, the streamwise component $\theta$ is defined as positive following the flow along the circular path centred on the centre of the circular bend tip, and $Y$ is defined as for the Cartesian system.

### *3. Data Reduction*

[6], [8], [9] demonstrated the applicability of the presented stereoscopic PIV technique in details. (see also [7] and [10]). The 3D PIV measurements are obtained from the combination of two 2-dimensional vector fields; from the processed vector fields, the instantaneous three-dimensional velocity field can be reconstructed. Matlab homemade reconstruction software was developed at the EPFL-LTT. The readers are referred to [7] for data reduction details.

In addition to the mean-velocity field, the normal and shear stress quantities of the flow are required to evaluate numerical codes. In order to obtain PIV measurements in these forms, the statistical distribution of the velocity components is determined in identical spatial windows from a series of instantaneous PIV measurements. From these statistical distributions, the ensemble average and the statistical central moments are calculated to determine the desired mean-velocity field and Reynolds stresses.

## 4. RESULTS AND DISCUSSION

The objectives of the present paper are to determine the influence of a film-cooling flow extraction on the flow fields upstream, inside and downstream of the bend region, and to provide new measurements of flow between ribs for CFD validation. The following are data and discussion on these topics.

### *1. Flow in the upstream leg*

A comparison of velocity components in the developed flow region of a similar coolant passage was presented by [11]. The measurements showed that the flow with a 45-deg rib arrangement, differs from the flow in a similar passage, with a 90-deg rib arrangement [12]. With 90 deg ribs, a developed flow condition in terms of mean velocity and turbulent kinetic energy was achieved after 3 rib modules. The flow in the passage with 45° rib arrangement requires a longer development length; at least 8 rib modules are needed to achieve a developed flow condition for the mean velocity components, and 12 rib modules are required for the turbulent kinetic energy of the flow. In the present configuration, 18 rib-modules are placed in the upstream leg, to produce a developed flow field before the 180-deg bend. The analysis of the developed flow characteristics in the baseline configuration was presented in [7] Figure 3, for the obvious reason of space in this paper, the Figure 3 is not plotted here, nor the same figure for the *hole* configuration. However the major results can be summarised as follow: The flow in the baseline configuration has shown to be developed in the upstream $16^{th}$ rib module, and the periodicity going with this developed state is extending up to the bend inlet. Instead, in the *hole* configuration, the flow in the $16^{th}$ rib module has already undergone the bend influence, the streamwise velocity variations reach 15% at the bend inlet location. The influence of the extraction in the configuration shows to extend upstream of the extraction region.

## 2. ***Flow in the bend region***

The flow in the upstream leg developed region of 180deg cooling channels has already been described by [12] and [7]. It is strongly influenced by the ribs on both opposite walls, yielding in two counter rotating vortices, both occupying half of the cross section. Figure 2 gives a comparison of both the baseline and the *hole* configurations described previously. Mean streamwise velocity contours and secondary flow vectors obtained at $\theta$=0, 45, 90, 135 and 180 deg in the bend are presented. These average velocity results were obtained from 1250 full-field data sets. For this set of results, the orientation of the view is always into the oncoming flow, with the web at the left-hand side of the figure.

The major difference occurs when comparing the secondary flow motion. The upper vortex ($Y$>0.5) occupies 70% of the cross section in the case of extraction. The counter-rotating vortex induced by the bottom ribs only occupies the $Y$<0.3 area. The streamwise component is also influenced by this asymmetry, showing a high velocity zone in the upper part.

The flow in the bend region is more complex than in the ribbed region. The flow in the bend starts with the secondary structure from the ribs at $\theta$=0deg. At $\theta$=0deg, the streamwise velocity distribution and the secondary flow patterns in the centre region show the effects of the bend (Figure 2). The streamwise flow near the inner web has begun to accelerate, indicating that this flow has entered the bend region. The secondary flow pattern is symmetrically distributed compared to a mid plane ($Y$=0.5) for the baseline configuration, whereas in the *hole* configuration, the secondary flow near the outer wall is mainly directed towards the bottom wall. The main impact is the inclusion of a high streamwise velocity core in the channel centre region. Note that near the web of both configurations, all the secondary flow vectors are toward the web in both cases.

At $\theta$=45deg, the streamwise velocity increases to more than 2 near the inner web, and has a small region of negative velocities in the lower outside corner region. The high streamwise velocity near the inner web is compatible with the conservation of angular momentum in the bend region. The secondary flows are very different from the baseline case, to the *hole* case. In the latter, instead of the four Dean vortices present in the baseline case, only two counter-rotating vortices occur. They have the same rotating direction as the two baseline case upper vortices, and their size are approximately twice bigger. Note that near the web, the secondary flow vectors are directed away from the web in both configurations.

At $\theta$=90deg, the streamwise velocities of the flow have decreased near the web. The size of the region near the web where the secondary flow is directed away from the web has increased. The upper baseline case secondary cell seen at 45deg continues, but the lower cell has disappeared. The two *hole* case secondary cells are still present, but their locations have been strongly modified by the bend induced flow.

At $\theta$=135deg, the flow has separated from the web and the streamwise velocities are negative. The streamline velocity contours are similar for both configurations. The streamwise velocity has a negative value near the outer wall, indicating a small recirculation cell. The *hole* case values are a bit smaller; this is due to the mass flow extraction through the first two holes in the bend. The average position of the baseline

vortex cell has moved toward the web, and the secondary flow is generally away from the web. The two *hole* case vortices continue to develop.

At $\theta$=180deg, a small region of recirculation occurs near the web and the lower wall. The rib induced secondary flow motion is redeveloping. The streamwise profiles are very similar in both cases; the effect of the flow extraction is, however, increasing in the *hole* case, yielding smaller streamwise magnitudes. Note that the highest streamwise velocities have moved from near the web to the outer half of the passage, and are 1.5 to 2.0 times the bulk velocity. The secondary flow is very different in the *hole* configuration; the flow goes from the top to the bottom wall along the web, crosses the channel up to the top outer wall, and goes down to the bottom wall along the outer wall. This phenomenon is similar to the upper half of the baseline secondary flow motion.

Downstream of the bend, the secondary flows are redeveloping, having a similar shape to the secondary flow in the upstream leg. The streamwise flow hasn't recovered from the bend effect. $1D_H$ downstream of the bend, the recirculating cell has disappeared in the baseline configuration, but is still present in the *hole* case. Further downstream ($3.6D_H$), the flow has almost recovered from the bend domination, the streamwise and secondary profiles are similar to the inlet profiles, except for the symmetry around the web, due to the rib symmetrical placement each side of the web. The *hole* configuration streamwise velocity magnitude, has also decreased because of the massflow extracted upstream.

## 3. ***Flow in the downstream leg***

Downstream of the bend is another region with relatively large variations in heat transfer. Figure 3 presents streamwise velocity contours of the downstream turn region, and gives further details of the flow characteristics in the streamwise direction. Corresponding secondary flow measurements are presented in Figure 2. The centre part of the channel is plotted ($0.3<Y<0.7$).

The streamwise velocity component recovers from the bend effect quite similarly in the baseline and the *hole* configurations. The flow homogenises in the spanwise direction as $X$ increases, the rib induced effects becoming preponderant. $4D_H$ downstream of the bend, the streamwise velocity magnitude is 30% lower in the *hole* than in the baseline configuration, this is due to the massflow lost in the upstream holes (~25% of $Q_{in}$ lost). As described in [7] the bend induced flow leads to a high non-homogeneity at the downstream leg inlet ($\theta$=180deg). The high-speed region ($U_\theta/U_b>1$) occupies the outer half part of the duct ($Z<-0.6$) and extends up to $X>2$. Near the web, a recirculating zone appears for $0.3<Y<0.7$ in the baseline configuration, whereas in the *hole* case, it doesn't appear for $Y$=0.7 and is only present at the very web tip for $Y$=0.5. This confirms the trend observed in Figure 2, that the entire flow field is displaced toward the bottom wall.

Except for the magnitude differences due to the extraction, both streamwise velocity profiles recover from the bend in the same manner, and the streamwise velocity shape in the centre part of the duct is not very sensitive to the extraction. The extraction influence is mainly noticeable in the secondary flow profiles.

## 5. CONCLUSIONS

Three-dimensional velocity measurements were obtained in a two-legged blade coolant passage model with ribs orientated 45 deg to the passage. The model length, the rib locations and the geometry of the web between the coolant passage legs, was representative of gas turbine cooling designs. Here is presented a comparison between two similar configurations, one is a baseline, the second one is provided with bleeding holes, simulating the holes for external film cooling of blades.

Adding bleeding holes, and having a high ratio between the channel inlet mass flow and the extracted mass flow, strongly influence the flow in the 2-legged cooling channel. It modifies the flow field in the entire test section, in the region where the extraction occurs, but also far upstream in the first leg of the channel. The influence on the streamwise velocity profiles is sensitive, but the greatest influence occurs on the secondary flow motions. The secondary flow moves from its symmetrical shape, in the baseline case, to a strongly asymmetrical shape in the *hole* case, as some part of mass flow is ejected from the channel. The streamwise symmetrical profile is unbalanced toward the wall with extraction, and the symmetry plane ($Y$=0.5) is displaced downward of about 20% of $D_H$. The secondary flow has to adapt to the streamwise conditions, and as a consequence is highly modified. All along the channel, the lower parts of the baseline secondary flow motion have almost disappeared, and the upper parts have been scaled by a factor 1.5 in the $Y$ direction. This asymmetry will probably strongly modify the heat transfer coefficient distribution on the ribbed surfaces.

The unsteady character of the flow may require time dependent numerical techniques to accurately simulate the flow. The area near the web, and probably upstream of the bend is likely to have large variations in heat transfer, due to the high variations in streamwise velocity, and may produce hot and cold spots, and possibly increased stresses with their thermal gradients.

## 6. ACKNOWLEGDGEMENTS

This study was funded by the Swiss Office of Science in cooperation with the BriteEuram Internal Cooling of Turbine Blades project (contract number: BRPR-CT97-0600, project number: BE97-4022).

## 7. REFERENCE

1. Byerley, A.R., Jones, T.V. and Ireland, P.T. (1992). *Internal cooling passage heat transfer near the entrance to a film cooling hole: Experimental and computational results*. Proceedings of the International Gas Turbine & Aeroengine Congress & Exhibition. Cologne, Germany. 1992. ,92-GT-241.
2. Shen, J.R., Wang, Z., Ireland, P.T. and Jones, T.V. (1996). *Heat transfer enhancement within a turbine blade cooling passage using ribs and combinations of ribs with film cooling holes.* Journal of Turbomachinery, 118 July 1996, 428-434.
3. Lourenco, L.M. (1988). *Some Comments on Particle Image Displacement Velocimetry*. In: *Lecture Series* (Von Karman Institute for Fluid Dynamics), Vol. 06.
4. Prasad, A.K. and Adrian, R.J. (1993). *Stereoscopic Particle Image Velocimetry Applied to Liquid Flows.* Experiments in Fluids, 15 , 49-60.

5. Westerweel, J. and Nieuwstadt, F.T. (1991). *Performance Tests on 3-Dimensional Velocity Measurements with a Two-Camera Digital Particle-Image-Velocimeter*. In: *Laser Anemometry* ), Vol. 1, 349-355.
6. Schabacker, J. and Bölcs, A. (1996). *Investigation of Turbulent Flow by means of the PIV Method*. Proceedings of the 13th Symposium on Measuring Techniques for Transonic and Supersonic Flows in Cascades and Turbomachines. Zurich, Switzerland. 1996.
7. Chanteloup, D. and Bölcs, A. (2001). *PIV investigation of the flow characteristics in 2-leg internal coolant pasages of gas turbine airfoils*. Proceedings of the Euroturbo, European conference on turbomachinery fluid dynamics and thermodynamics. Firenze, Italy. 2001.
8. Schabacker, J., Bölcs, A. and Johnson, B.V. (1998). *PIV investigation of the flow characteristics in an internal coolant passage with two ducts connected by a sharp 180° bend*. Proceedings of the International Gas Turbine & Aeroengine Congress & Exhibition. Stockholm, Sweden. 1998. ,98-GT-544.
9. Schabacker, J. (1998). *PIV investigation of the flow characteristics in an internal coolant passages of gas turbine airfoils with two ducts connected by a sharp 180° bend*. In: *Thesis* (Ecole Polytechnique fédérale de Lausanne), Vol. n°1816.
10. Raffel, M., Willert, C.E. and Kompenhans, J. (1997). *Particle Image Velocimetry. A practicle guide* (Springer), ISBN 3-540-63683-8.
11. Bohnof, B., Schabacker, J., Parneix, S., Leusch, J., Johnson, B.V. and Bölcs, A. (1998). *Experimental and numerical study of developed flow and heat transfer in coolant channels with 45 and 90 degree ribs*. Proceedings of the Turbulent heat transfer II. Manchester, UK. 1998. ,99-GT-123.
12. Schabacker, J., Bölcs, A. and Johnson, B.V. (1999). *PIV investigation of the flow characteristics in an internal coolant passage with 45° rib arrangement*. Proceedings of the International Gas Turbine & Aeroengine Congress & Exhibition. Indianapolis, Indiana, USA. 1999. ,99-GT-120.

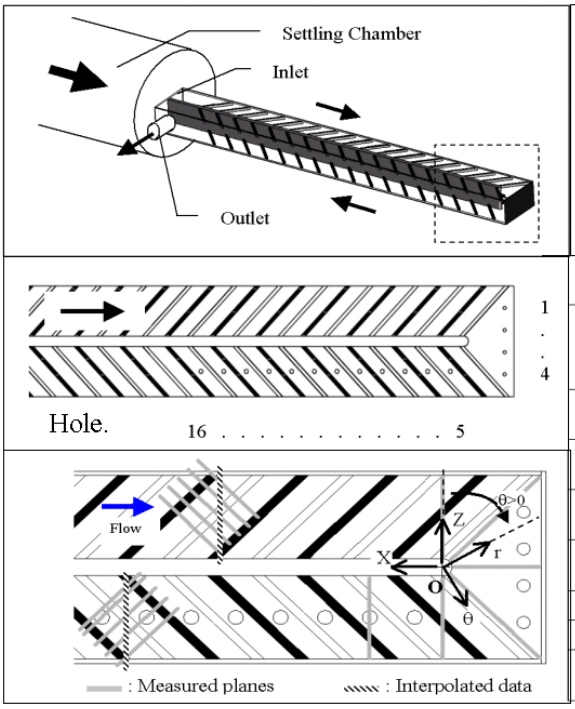


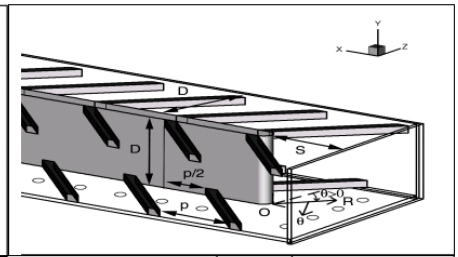


| | | |
|---|---|---|
| Test section length | L | 20 $D_h$ |
| Height & Width of passage legs | D | 1 $D_h$ |
| Bend cross section | S | 1 $D_h$ |
| Length of divider plate | | 19 $D_h$ |
| Thickness of divider plate | B | 0.2 $D_h$ |
| Rib cross-section | | 0.1 $D_h^2$ |
| Rib pitch | P | 1 $D_h$ |
| Rib height | e | 0.1 $D_h$ |
| Rib angle of attack | | 45deg |

*Figure 1 The internal coolant passage test facility and turn region details. Measurement sections. The symbols represent the measurement lines (Y direction) that will be analysed in the next sections (Figure 2).*

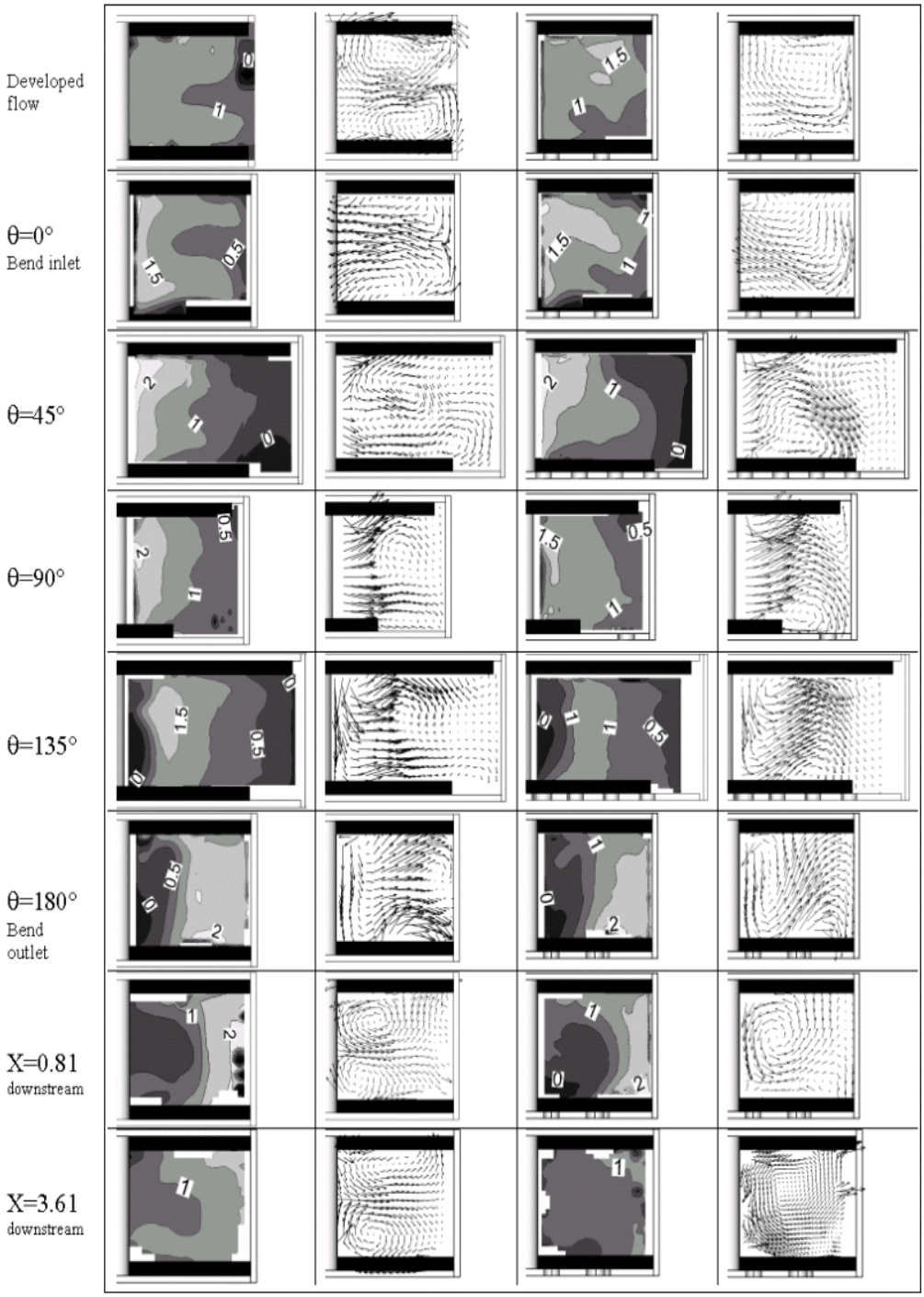


*Figure 2: Mean streamwise velocity contours and secondary flow vectors obtained at $\theta$=0, 45, 90, 135 and 180 deg in the bend. The contour lines values, $U_\theta$ , are plotted on the figures ($U_\theta$ / Ub).*

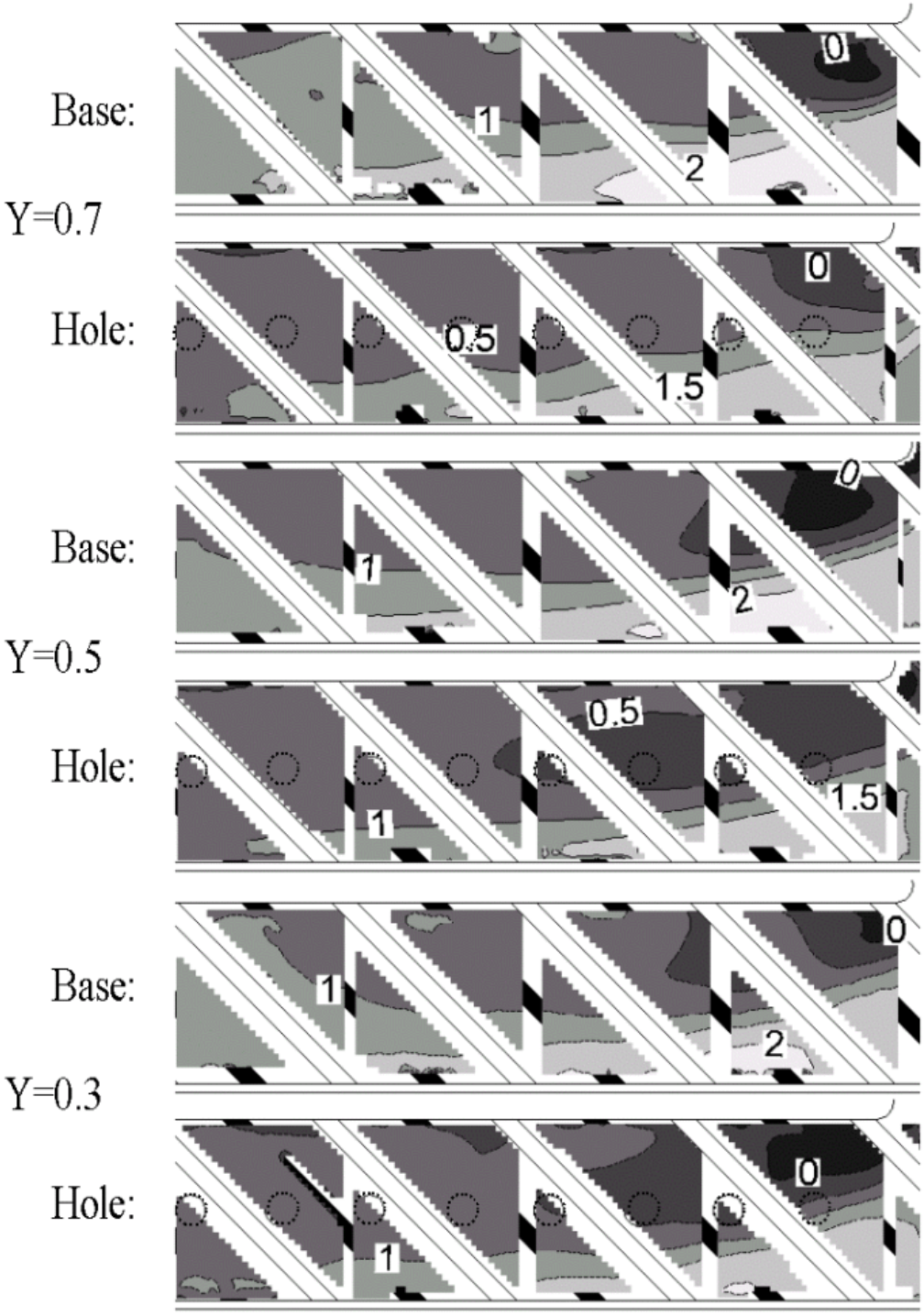


*Figure 3: streamwise velocity contours immediately downstream of the bend, 0.0 < X < 4.0 at three distances from the bottom wall (U / Ub).*